

GAMMA-RAY BURST PHYSICS WITH GLAST

N. OMODEI

*INFN sez. Pisa,
Edificio C - Polo Fibonacci -
Largo B. Pontecorvo, 3 PISA,
E-mail: nicola.omodei@pi.infn.it*

The Gamma-ray Large Area Space Telescope (GLAST) is an international space mission that will study the cosmos in the energy range 10 keV-300 GeV, the upper end of which is one of the last poorly observed region of the celestial electromagnetic spectrum. The ancestor of the GLAST/LAT was the Energetic Gamma Ray Experiment Telescope (EGRET) detector, which flew onboard the Compton Gamma Ray Observatory (CGRO). The amount of information and the step forward that the high energy astrophysics made thanks to its 9 years of observations are impressive. Nevertheless, EGRET uncovered the tip of the iceberg, raising many questions, and it is in the light of EGRET's results that the great potential of the next generation gamma-ray telescope can be appreciated. GLAST will have an imaging gamma-ray telescope, the Large Area Telescope (LAT) vastly more capable than instruments flown previously, as well as a secondary instrument, the GLAST Bursts Monitor, or GBM, to augment the study of gamma-ray bursts. Gamma-Ray Bursts (GRBs) science is one of the most exciting challenges for the GLAST mission, exploring the high energy emission of one of the most intense phenomena in the sky, shedding light on various problems: from the acceleration of particles to the emission processes, to more exotic physics like Quantum Gravity effect. In this paper we report the work done so far in the simulation development as well as the study of the LAT sensitivity to GRB.

1. The Gamma-ray Large Area Space Telescope (GLAST)

The main instrument on board the GLAST satellite is the Large Area Telescope (LAT). It is a pair conversion telescope, like EGRET, but the detectors will be based on solid-state technology, obviating the need for consumables and greatly decreasing instrument dead-time. The LAT comprises an array of 16 identical "tower" modules (see Fig. 1), each with a tracker (Si strips), a calorimeter (CsI with PIN diode readout) and a Data Acquisition (DAQ) module. The towers are surrounded by a finely segmented anti-coincidence detector (ACD), made by plastic scintillator, while the support structure is an aluminum strong-back "Grid" with heat

pipes for transport of heat to the instrument sides.

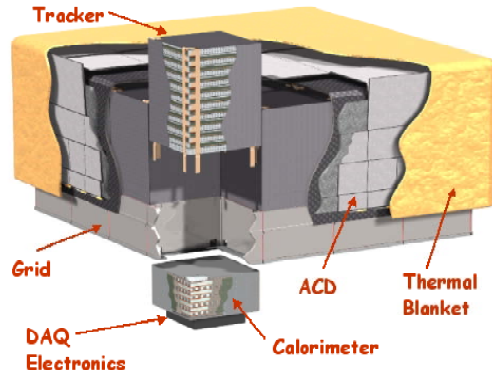


Figure 1. The LAT instrument components: The ACD is the anti coincidence detector, for the background rejection. CAL is the calorimeter which provide measurements on the energy. The Tracker is the complex tracker system based in Si Strips Detectors. The Grid has the structural function of hinging the towers. The DAQ electronic is mounted below. The thermal blanket covers the full instrument providing heat insulation.

LAT will have superior area, angular resolution, field of view, and dead time that together will provide a factor of 40 or more advance in sensitivity, covering the energy range between 20 MeV and 300 GeV. Aside from the main instrument LAT, a secondary instrument, the GLAST Burst Monitor (GBM), is foreseen. With the LAT and GBM, GLAST will be a flexible observatory for investigating the great range of astrophysical phenomena best studied in high energy gamma rays. NASA plans to launch GLAST in early 2007 from Kennedy Space Flight Center.

2. Gamma-Ray Bursts

Gamma-Ray Bursts (GRBs), are short and intense pulses of high energy radiation whose duration varies from fractions of a second to several hundred of seconds. They were serendipitously discovered in the sixties by the four Vela satellites¹ and their extragalactic origin were directly observed by the Italian-Dutch satellite BeppoSAX (1996-2002) measuring the first X-Ray afterglow². BATSE (Burst And Transient Source Experiment) detector on board the CGRO observing more than 2700 burst, in its 9 years of observations while EGRET, mainly due to its small effective area, observed only

few photons coming from GRBs³, and the high energy emission from GRB is still puzzling and enigmatic^{4,5,6}.

Several Gamma-Ray Bursts source models have been developed, starting from different hypothesis and describing different scenarios. One of the most creditable model is the *fireball* model introduced by Piran, 1999⁷, starting from the evolution of a relativistic expanding shell⁸. In the most schematic view of the fireball model, a hidden central engine emits “shells” of matter (plasma) into the interstellar medium with relativistic bulk Lorentz factors (for a complete review of the Fireball model, see also⁹). If the central engine emits shells with different velocities, a faster shell can reach a slower one producing a shock. The dissipated energy can be used both to accelerate particles and to generate magnetic fields. Charged particles in magnetic fields lose energy via synchrotron emission and, eventually, can boost the synchrotron photons via inverse Compton (IC) scattering producing high energy photons. We have developed a GRB source model (details in¹⁰) based on the Fireball model, that can be used within the GLAST/LAT simulation framework¹¹ for studying the response of the LAT detector to GRB signal. In practice, we normalize GRB fluences to the BATSE observed distribution¹², and we extrapolate to LAT energies on the basis of common physical principle such as the synchrotron radiative process and the inverse Compton scattering. Here we are interested in two main features: the synchrotron cut-off due to the finite value of the Lorentz factor at which electrons are accelerated^{13,14}, and the inverse Compton component, in particular, how the sensitivity of the LAT instrument varies with respect to the inverse Compton emissivity.

2.1. *Measurement of the high energy cut-off*

In our simulation we assume as initial distribution of electrons a power law between γ_{min} and γ_{max} with power law index $-p$, and that each shock produced a pulse. The maximum Lorentz factor of the accelerated electrons (γ_{max}) determines a cut-off at high energies, so that we adopt a parameterized function for the GRB spectrum due to pure synchrotron emission. For fast cooling regime, which is the case of GRB: $P(E) = Exp(-E/E_M)(E/E_c)^{1/3}$ for energy less than the typical cooling energy (E_c); $P(E) = Exp(-E/E_M)(E/E_c)^{-1/2}$ for energies between the cooling energy and the “minimum” energy $E_c < E < E_m$; and $P(E) = Exp(-E/E_M)(E_m/E_c)^{-1/2}(E/E_m)^{-p/2}$ for energies higher than the minimum energy. Notice that for a γ_{max} large enough (as consequence,

large E_M) the spectra reduces to the usual broken power law proposed by Sari et al.(1998)¹⁵. Nevertheless, there is a linear relation between the cut-off energy E_M , expressed in GeV, and the Lorentz factor of the emitting shell Γ , given, numerically by $E_M = 2.5 \Gamma/100$. Measuring the high energy cut-off at GeV energies one can measure the (average) Lorentz factor of the expanding shells. In Fig. 2 we simulated a GRB with a BATSE fluence $3.17 \times 10^{-5} \text{ erg/cm}^2$, which generates 1220 photons above 100 MeV, whose result in 408 triggered and reconstructed photons. The data have been fitted with a power law, and with a power law with an exponential cut-off. The chi-square test gives the probability for the different models, showing that the simple power law function is clearly unsatisfactory, while the power law with the exponential cut-off is in agreement with the (simulated) data. The cut-off estimated energy is $5.5 \pm 1.5 \text{ GeV}$.

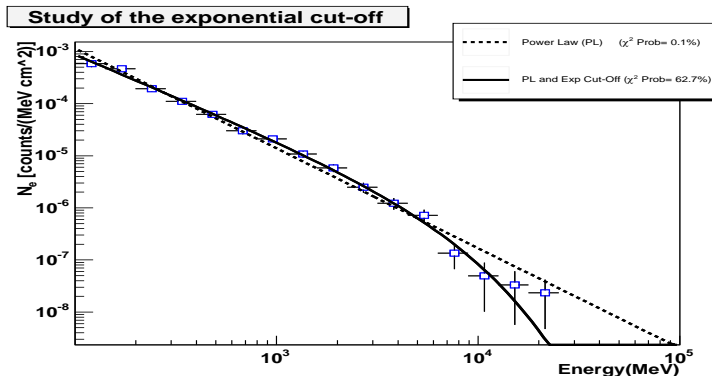


Figure 2. Study of the high energy cut-off. The simulated data have been produced using the GRB model forcing a high energy cut-off at 4.5 GeV. The reconstructed data are displayed in the plot and have been fitted with a power law distribution (dashed line), and with a power law distribution with an exponential cut-off (solid line). In the legend the values of the χ^2 test denote the probability to obtain a greater χ^2 by chance, for the two different models. The cut-off estimated energy is $5.5 \pm 1.5 \text{ GeV}$.

2.2. The inverse Compton component

The inverse Compton process boosts up the synchrotron photons by means of scattering against the high energy electrons in “Self Synchrotron Compton” or SSC configuration. The electron distribution is a power law and the most probable scattering is between the lowest energetic electrons (whose

energy is $\approx E_m$) against the synchrotron spectrum. In the relativistic case (when the energy of the electrons is much more greater than their rest mass) the photons are up scattered by a quantity γ^2 where the γ is the Lorentz factor of the electrons. In GRB, the peak of the synchrotron spectrum (E_{peak}) is typically of the order of hundreds of keV, and the minimum Lorentz factor of the accelerated particles is $\gamma \approx 10^2$: the typical IC peak is hence expected to be around GeV energies. The typical signature of the IC is the presence of a maximum in the $\nu F(\nu)$ spectrum (or $E^2 N(E)$) in the GeV energy range. We scale the inverse Compton component by means of a parameter τ which represents the intensity of the peak of the inverse Compton component (the height of the IC bump of the $\nu F(\nu)$ spectrum) relative to the intensity of the synchrotron component (the height of the synchrotron bump of the $\nu F(\nu)$ spectrum). Fig. 3 shows the simulation in case of $\tau = 1$, which represents, roughly, the same amount of energy in the synchrotron emissions as in the SSC emission.

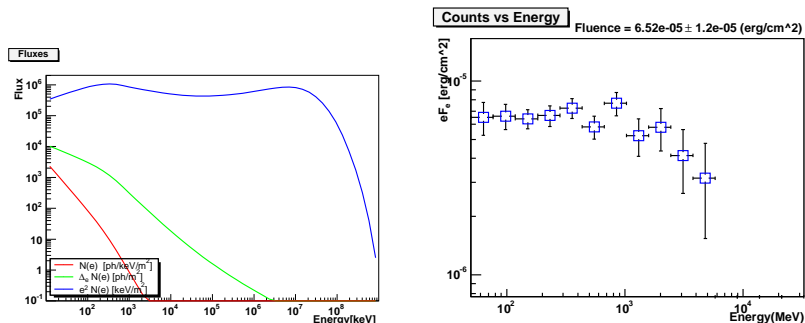


Figure 3. Detecting the inverse Compton component. Left: spectral energy distribution of an intense GRB (between 20 keV and 1 MeV its fluence is $F = 5 \times 10^{-5} \text{ erg/cm}^2$) with $\tau = 1$. Right: same burst viewed by the LAT detector. The peak of the inverse Compton component (of the $E F(E)$ spectrum) is at $\approx 2 \text{ GeV}$, detectable by the LAT detector.

2.3. GLAST sensitivity for GRB

As final exercise, we compute the sensitivity of the LAT detector for GRB. We have simulated 10000 bursts with different inverse Compton components varying the parameter τ uniformly from 0 (pure synchrotron spectrum) to 10 (high inverse Compton component). Each burst has been normalized

between 20 keV and 1 MeV to the BATSE fluence distribution. In this computation we consider the effective area flat above 100 MeV. For normal incidence photons we consider $A_{on-axis} = 0.84 \text{ m}^2$, and $A_{off-axis} = 0.05 \text{ m}^2$ (which corresponds to an incident direction of 67° degrees from the normal). The distribution of the the fluence in the BATSE energy range versus the number of generated photons above 100 MeV for 10000 simulated bursts is shown in left panel of Fig. 4. The two horizontal lines represent the burst detection thresholds for on-axis and off-axis incident directions: they represent the number of photons per square meter in order to have at least 5 photons detected by the LAT: these are the required number of events in order to recognized a spatial-temporal cluster needed to detect a transient signal¹⁶. The efficiencies in the GRBs detection are 89.4% for on-axis and 46.9% for off-axis, as depicted in the right panel of Fig.4. Considering that BATSE has detected 550 bursts per year over 4π and the field of view for on-axis and off-axis detection is equal to $2\pi \cdot 0.2$: we predict that the LAT will see from 30 to 50 bursts on-axis per year, (10 to 30 for off axis detection) depending on their spectral features. Left panel of Fig. 5 shows

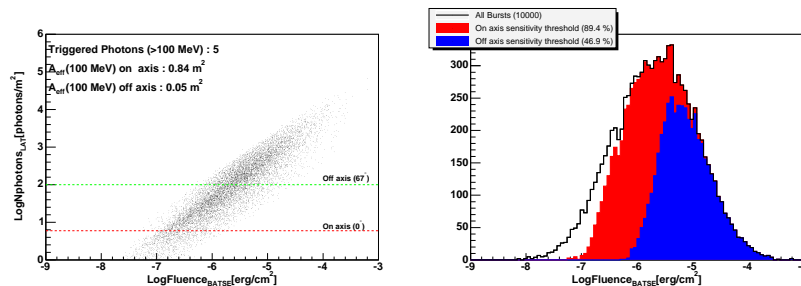


Figure 4. Left: number of generated photons per square meter above 100 MeV versus the fluence in the BATSE energy range. The two horizontal lines represent the burst detection thresholds for on-axis and off-axis observation. They represent the number of photons per square meter to generate in order to have at list 5 photons detected by the LAT. They are at $\log(5/0.84) = 0.77$ for on-axis detection, and $\log(5/0.05) = 2$ for off-axis detection. The dots above the thresholds are detectable bursts. Right: detectable bursts ratio (filled histograms, for on-axis and off-axis) with respect to the total number of burst generated (empty histogram).

the fraction of GRBs detected as a function of the parameter τ , for on-axis detection and for off-axis detection.

Another interesting study that can be done using this approach, is to determine the distribution in redshift, and the highest observable redshift

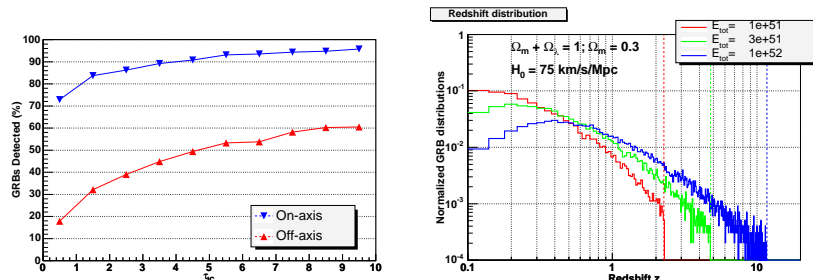


Figure 5. Fraction of detected GRBs as a function of the parameter τ . The situation of pure synchrotron spectrum yields a detection percentage of 73% for on-axis detection, and 18% for off-axis detection. For high inverse Compton component the on-axis detection approaches the 96% of the total generated bursts, while, for off-axis detection, the 61%. Simulated redshift distribution for different values of the intrinsic energy, and a given cosmology.

assuming GRB as standard candle^{17,18,19}. Assuming a flat universe ($\Omega = \Omega_m + \Omega_\lambda = 1$, with $\Omega_m = 0.3$, and $H_0 = 0.71_{-0.03}^{+0.04}$ km/s/Mpc)^{20,21} one can compute the redshift of a burst given the fluence F and assuming different values for the intrinsic energy E_{tot} :

$$z(F) = \frac{8 c H_0 \sqrt{\pi E_{tot} F \Omega_m} + E_{tot} H_0^2 \Omega_m}{16 \pi c^2 F} \quad (1)$$

Right panel of Fig. 5 shows the distribution of redshift for three different values of the emitted energy. The intrinsic energy E_{tot} is assumed to be corrected by the beaming angle, so that even if the “isotropic equivalent” energy covers almost three decades of energy (10^{51} erg- 10^{54} erg), the emitted energy is a narrow distribution centered at 1.3×10^{51} erg. We can conclude that, depending on the Gamma-Ray Bursts energetic reservoir, GLAST will be able to scan the universe up to early epoch ($z=10$ for an intrinsic luminosity of 10^{52} ergs, $z=5$ for 10^{51} and $z=2$ for 3×10^{51} erg).

3. Conclusions

GLAST, the new generation gamma ray telescope, represents a big step forward in terms of technology and development, which will be translated in an enormous amount of new science, including discoveries. GRB are suitable sources for the GLAST mission: the LAT detector will observe the purely observed high energy range, adding informations on the acceleration of particles and on the radiative processes that allows production of gamma-rays up to GeV energies. In this article we simulated GRBs using a model

that allows the flux normalization at BATSE energies and extrapolates the spectrum up to LAT energies, using the synchrotron model prescription. We shown that LAT is sensitive to the synchrotron cut-off: LAT will be able to reconstruct this spectral feature with statistic significance. We also simulate the inverse Compton component with a parametric, but accurate, spectral function. The presence of such component enhance the spectrum at LAT energy as well as determines a second bump in the $\nu F(\nu)$ spectrum. We finally investigate the sensitivity of the LAT to GRBs, computing the ratio of bursts which are independently detectable by the LAT instrument. LAT will see tens of bursts per year, depending on their spectral features. Gamma-Ray Bursts science with GLAST will definitely be one of the most exciting adventures, especially thanks to the Large Area Telescope.

References

1. R. W. Klebesadel, I. B. Strong, and R. A. Olson, *Ap. J. Lett.*, **182**:L85+, (1973).
2. E. Costa, *et al.*, *Nature*, **387**:783–785, (1997).
3. B. L. Dingus, *Astrophys. & Space Sci.*, 231:187–190, (1995).
4. K. Hurley, *et al.*, *Bulletin of the American Astronomical Society*, **26**:881–+, (1994).
5. K. Hurley, *et al.*, *IAUCirc*, **5940**:1–+, (1994).
6. M. M. González, *et al.*, *Nature*, **424** :749–751, (2003).
7. T. Piran, *Physics Reports*, **314**:575–667, (1999).
8. R. D. Blandford and C. F. McKee, *Physics of Fluids*, **19** :1130–1138, (1976).
9. Piran, T., *Reviews of Modern Physics*, **76**, 1143, (2005).
10. N. Omodei. Modeling, simulation and optimization of the detection of Gamma-Ray Burst with GLAST, *Ph.D. Thesis*, (2005).
11. P. Boinee, *et al.*, In *Science with the New Generation of High Energy Gamma-Ray Experiments : Between Astrophysics and Astroparticle Physics*, (2003).
12. W. S. Paciesas, *et al.*, *Ap. J. Supp.*, **122**:465–495, (1999).
13. O. C. de Jager and A. K. Harding, *Ap. J.*, **396**:161–172, (1992).
14. O. C. de Jager, *et al.*, *Ap. J.*, **457**:253–+, (1996).
15. R. Sari, T. Piran, and R. Narayan, *Ap. J. Lett.*, **497**:L17+, (1998).
16. J. Cohen-Tanugi *et al.*, *astro-ph/0301356*
17. D. A. Frail, *et al.*, *Ap. J. Lett.*, **562**:L55–L58, (2001).
18. J. S. Bloom, D. A. Frail, and S. R. Kulkarni *Ap. J.*, **594**:674–683, (2003).
19. G. Barbiellini, *et al.*, *Mon. Not. RAS*, **350** :L5–L8, (2004).
20. C. L. Bennett, *et al.*, *Ap. J. Supp.*, **148**:1–27, (2003).
21. F. K. Hansen, A. Balbi, A. J. Banday, and K. M. Górski, *Mon. Not. RAS*, **354**:905–912, (2004).